Computer Methods in Applied Mechanics and Engineering 199 (2010) 2559–2570

Contents lists available at ScienceDirect

Computer Methods in Applied Mechanics and Engineering

journal homepage: www.elsevier.com/locate/cma

Mixed stabilized finite element methods in nonlinear solid mechanics Part I: Formulation

M. Cervera *, M. Chiumenti, R. Codina

International Center for Numerical Methods in Engineering (CIMNE), Technical University of Catalonia (UPC), Edificio C1, Campus Norte, Jordi Girona 1-3, 08034 Barcelona, Spain

ARTICLE INFO

Article history:
Received 22 July 2009
Received in revised form 9 March 2010
Accepted 13 April 2010
Available online 18 April 2010

Keywords:
Mixed finite element interpolations
Stabilization methods
Algebraic sub-grid scales
Orthogonal sub-grid scales
Nonlinear solid mechanics

ABSTRACT

This paper exploits the concept of stabilized finite element methods to formulate stable mixed stress/displacement and strain/displacement finite elements for the solution of nonlinear solid mechanics problems. The different assumptions and approximations used to derive the methods are exposed. The proposed procedure is very general, applicable to 2D and 3D problems. Implementation and computational aspects are also discussed, showing that a robust application of the proposed formulation is feasible. Numerical examples show that the results obtained compare favorably with those obtained with the corresponding irreducible formulation.

1. Introduction

The term *mixed methods* has been used in the finite element method literature since the mid 1960s to denote formulations in which both the displacement and stress fields are approximated as primary variables [1]. Despite the doubtless interest of mixed methods from the theoretical point of view, their practical application is greatly outnumbered by the implementation of *irreducible methods,* in which only the displacement field is considered primary variable of the problem and the stress field is obtained *a posteriori* by differentiation.

However, there are several fields of application in computational solid mechanics in which mixed methods are well established and regularly used in practice. For instance, it is well known that standard irreducible low order finite elements perform miserably in nearly incompressible situations, producing solutions which are almost completely locked by the incompressibility constraint. Remedies for this undesirable behavior have been actively sought for decades. In fact, the purely incompressible problem (Stokes problem) does not admit an irreducible formulation and, consequently, a mixed framework in terms of displacements and pressure is necessary for these situations. Over the years, and particularly in the 1990s, different strategies were proposed and tested to reduce or avoid volumetric locking and pressure oscillations in finite element solutions with different degrees of success [2–14]. Many of these methods, while resembling displacement methods, have been shown to be equivalent to more general mixed methods.

Another common application of mixed methods is plate bending and other fourth order problems [5,15–17]. Here, the motivation is the avoidance of C^1-continuity in the definition of the interpolation functions, required if the primal variational functional is used. Alternatively, the mixed functional only involves second derivatives and, after integration by parts, C^0-continuous elements may be used. Another alternative is the use of non-conforming elements.

The reasons for the limited popularity of mixed methods in computational solid mechanics are twofold: computational cost and lack of stability [18–20]. On one hand, because mixed methods approximate both displacements and stresses simultaneously, the corresponding discrete systems of equations involve many more degrees of freedom than the corresponding irreducible formulations. Concurrently, the mixed system of equations is very often indefinite, which makes most of the direct and iterative solution methods inapplicable. These difficulties may be avoided with a suitable implementation. On the other hand, many choices of the individual interpolation fields for the mixed problem yield meaningless, not stable, results. This is due to the strictness of the inf-sup condition [19] when the standard Galerkin finite element method is applied straightforwardly to mixed elements, as it imposes severe restrictions on the compatibility of the interpolations used for the displacement and the stress fields. This difficulty, if not circumvented, is severely restrictive (see [21–23] for the analysis of admissible elements in linear elasticity).

In parallel, mixed methods have also been the focus of attention in computational fluid dynamics. In [24,25], the variational multiscale (VMS) formulation was proposed as a new way of circumventing the difficulties posed by the inf-sup condition. In the case of incompressible problems, the reasoning behind was not new, as it consisted of modifying the discrete variational form to attain control on the pressure field. The

* Corresponding author.
E-mail address: miguel.cervera@upc.edu (M. Cervera).

0045-7825/$ – see front matter © 2010 Elsevier B.V. All rights reserved.
doi:10.1016/j.cma.2010.04.006

result was the possibility of using equal order interpolations for displacements and pressures and to construct stable low order elements. Since then, the sub-grid concept underlying the VMS approach has been extensively and fruitfully used in fluid dynamics. In [26,27], the concept of orthogonal subscale stabilization (OSS) was introduced, which leads to well sustained and better performing stabilization procedures. The analysis of the formulation can be found in [28] for the linearized incompressible Navier–Stokes equations and, in subjects closer to the topic of this paper, in [29] for the stress–displacement-pressure formulation of the Stokes problem (equivalent to the linear elastic incompressible problem) and in [30] for Darcy's problem.

In previous works, the authors have applied *stabilized mixed displacement/pressure methods* (see [31–36]) to the solution of incompressible J_2-plasticity and damage problems with strain localization using linear/linear simplicial elements in 2D and 3D. These procedures lead to a discrete problem which is fully stable, free of pressure oscillations and volumetric locking and, thus, results obtained are practically *mesh independent*. This translates in the achievement of two important goals: (a) the position and orientation of the localization band is independent of the directional bias of the finite element mesh and (b) the global post-peak load-deflection curves are independent of the size of the elements in the localization band. Similar ideas have been used in [37–39].

In the present work we apply this approach in order to derive stable mixed stress–displacement and strain–displacement formulations using linear/linear interpolations in triangular elements and bilinear/bilinear interpolations in quadrilateral elements. It is noteworthy that, from the numerical point of view, the difficulties encountered in this problem are very different to those found in incompressible situations, analyzed in previous works. The treatment of the incompressible case in the stress/displacement formulation would require considering the pressure as an additional independent variable and appropriate stabilization techniques (see [29]). The incompressible limit will not be treated here, and the following formulation is limited to compressible nonlinear solid mechanics.

The basic motivation for this work is to show that the difficulties encountered when solving solid mechanics problems involving the creation and propagation of strain localization bands using standard elements and local constitutive models are due to *the approximation error inherent to the spatial discretization*, as well as to the *poor stability in the stresses and/or strains*. When using the basic, irreducible, formulation of the problem, the stresses (or strains), which are the variables of most interest for the satisfaction of the highly nonlinear constitutive behavior, are not the fundamental unknowns of the problem and they are obtained by differentiation of the displacement field, a process which entails an important loss of accuracy, particularly where strong displacement gradients occur. The local approximation error committed makes propagation of the localization bands strongly dependent on the finite element mesh used. Contrariwise, when using a mixed formulation in which the stress (or the strain) field is selected as primary variable, together with the displacement field, the added accuracy and stability achieved are enough to overcome the mesh dependency problem satisfactorily.

The outline of the present paper is as follows. In Section 2 the mixed stress/displacement finite element formulation for linear elasticity is summarized. The sub-grid scale approach is used to derive two stabilized formulations. Results concerning stability and convergence of these schemes are discussed. In Section 3 the stabilization is extended to nonlinear problems, proposing both stress–displacement and strain–displacement formulations. The later can be considered more suitable for the implementation of nonlinear constitutive models. Implementation and computational aspects are discussed next. Finally, some numerical benchmarks and examples are presented to assess the present formulation and to compare its performance with the standard irreducible elements. The problem of strain localization is discussed in a companion paper [40].

2. Mixed stabilized stress–displacement formulation in linear elasticity

2.1. Continuous problem

The formulation of the solid mechanics problem can be written considering the stress as an independent unknown, additional to the displacement field. In this case, the strong form of the continuous problem can be stated as: given a field of prescribed body forces $\mathbf{f}$ and a constant constitutive tensor $\mathbf{C}$, find the displacement field $\mathbf{u}$ and the stress field $\boldsymbol{\sigma}$ such that:

$$-\boldsymbol{\sigma} + \mathbf{C} : \nabla^s \mathbf{u} = 0 \qquad \text{in } \Omega \tag{1a}$$

$$\nabla \cdot \boldsymbol{\sigma} + \boldsymbol{f} = 0 \qquad \text{in } \Omega \tag{1b}$$

where Ω is the open and bounded domain of $\mathbb{R}^{n_{\dim}}$ occupied by the solid in a space of $n_{\dim}$ dimensions.

Eqs. (1a)–(1b) are subjected to appropriate Dirichlet and Neumann boundary conditions. In the following, we will assume these, without loss of generality, in the form of prescribed displacements $\mathbf{u}=\mathbf{0}$ on $\partial\Omega_u$, and prescribed tractions $\bar{\mathbf{t}}$ on $\partial\Omega_t$, respectively, being $\partial\Omega_u$ and $\partial\Omega_t$ a partition of $\partial\Omega$.

Multiplying by the test functions and integrating by parts the second equation, the associated weak form of the problem (Eq. (1a)–(1b)) can be stated as:

$$-\left(\boldsymbol{\tau}, \mathbf{C}^{-1} : \boldsymbol{\sigma}\right) + \left(\boldsymbol{\tau}, \nabla^s \mathbf{u}\right) = 0 \qquad \forall \boldsymbol{\tau} \tag{2a}$$

$$\left(\nabla^s v, \boldsymbol{\sigma}\right) = \left(v, \boldsymbol{f}\right) + \left(v, \ \bar{\mathbf{t}}\right)_{\partial\Omega_t} \qquad \forall v \tag{2b}$$

where $\mathbf{v} \in \mathcal{V}$ and $\tau \in \mathcal{T}$ are the test functions of the displacement and stress fields, respectively, and $(\cdot, \cdot)$ denotes the inner product in $L^2(\Omega)$, the space of square integrable functions in Ω. Hereafter, orthogonality will be understood with respect to this product. Likewise, $(\mathbf{v}, \bar{\mathbf{t}})_{\partial\Omega_t}$ denotes the integral of $\mathbf{v}$ and $\bar{\mathbf{t}}$ over $\partial\Omega_t$. For the sake of shortness, we will write $\mathrm{F}(\mathbf{v}) = (\mathbf{v}, \mathbf{f}) + (\mathbf{v}, \bar{\mathbf{t}})_{\partial\Omega_t}$ in the following. Eqs. (2a) and (2b) can be understood as the stationary conditions of the classical Hellinger–Reissner functional (see [41] for a description of a broader class of mixed methods).

The space of stresses $\mathcal{T}$ consists of symmetric tensors whose components are in $L^2(\Omega)$. If the weak form is written as indicated in Eq. (2a), the displacements and their test functions have to have components in $H^1(\Omega)$ (they and their derivatives have to be in $L^2(\Omega)$) and must vanish on $\partial\Omega_u$. This defines the space of displacements $\mathcal{V}$. However, it is also possible to integrate the second term in Eq. (2a), by parts, obtaining $(\tau, \nabla^s \mathbf{u}) = -(\nabla \cdot \boldsymbol{\tau}, \mathbf{u})$, and similarly for the left-hand-side of Eq. (2b). In this case, the components of the stresses have to have also the divergence in $L^2(\Omega)$, but the components of the displacement need to be only in $L^2(\Omega)$, not $H^1(\Omega)$. Similar to Darcy's problem, there are two possible functional settings for the linear elastic problem written in mixed form (see [30]). This is not essential for our discussion, although it has some implications in the treatment of boundary conditions on which we will not enter.

2.2. Galerkin finite element approximation

Let us now define the *discrete Galerkin* finite element counterpart problem as:

$$-\left(\boldsymbol{\tau}_h, \mathbf{C}^{-1} : \boldsymbol{\sigma}_h\right) + \left(\boldsymbol{\tau}_h, \nabla^s \mathbf{u}_h\right) = 0 \qquad \forall \boldsymbol{\tau}_h \tag{3a}$$

$$\left(\nabla^s \mathbf{v}_h, \boldsymbol{\sigma}_h\right) = \mathrm{F}(\mathbf{v}_h) \qquad \forall \mathbf{v}_h \tag{3b}$$

where $\mathbf{u}_h$, $\mathbf{v}_h \in \mathcal{V}_h$ and $\boldsymbol{\sigma}_h$, $\boldsymbol{\tau}_h \in \mathcal{T}_h$ are the *discrete* displacement and stress fields and their test functions, defined onto the finite element spaces $\mathcal{V}_h$ and $\mathcal{T}_h$, respectively. Note that the resulting system of equations is *symmetric* but *non-definite*. In all what follows, we will be interested in *continuous* finite element spaces $\mathcal{V}_h$ and $\mathcal{T}_h$ and, more specifically, in equal interpolation for stresses and displacements. Therefore, we may replace $(\boldsymbol{\tau}_h, \nabla^s \mathbf{v}_h)$ by $-(\nabla \cdot \boldsymbol{\tau}_h, \mathbf{v}_h)$, for all $\mathbf{v}_h \in \mathcal{V}_h$ and $\boldsymbol{\tau}_h \in \mathcal{T}_h$.

As it is well known, the stability of the discrete formulation depends on appropriate compatibility restrictions on the choice of the finite element spaces $\mathcal{V}_h$ and $\mathcal{T}_h$, as stated by the *inf-sup* condition [19]. According to this, standard Galerkin mixed elements with continuous *equal order* linear/linear interpolation for both fields are not stable. Lack of stability shows as uncontrollable oscillations in the displacement field that entirely pollute the solution. Fortunately, the strictness of the inf-sup condition can be avoided by modifying the discrete variational form, for instance, by means of introducing appropriate numerical techniques that can provide the necessary stability to the desired choice of interpolation spaces. The objective of this work is precisely to present stabilization methods which allow the use of equal order continuous interpolations for displacements and stresses.

2.3. Stabilized finite element methods

2.3.1. Scale splitting

The basic idea of the sub-grid scale approach [24] is to consider that the continuous unknowns can be split in two components, one coarse and a finer one, corresponding to different scales or levels of resolution. The solution of the continuous problem contains components from both scales.

For the solution of the discrete problem to be stable it is necessary to, somehow, include the effect of both scales in the approximation. The coarse scale can be appropriately solved by a standard finite element interpolation, which however cannot solve the finer scale. Nevertheless, the effect of this finer scale can be included, at least locally, to enhance the stability of the displacement in the mixed formulation.

To this end, the stress and the displacement fields of the mixed problem will be approximated as

$$\boldsymbol{\sigma} = \boldsymbol{\sigma}_h + \tilde{\boldsymbol{\sigma}}, \quad \mathbf{u} = \mathbf{u}_h + \tilde{\mathbf{u}} \tag{4}$$

where $\boldsymbol{\sigma}_h \in \mathcal{T}_h$ and $\mathbf{u}_h \in \mathcal{V}_h$ are the components of the stresses and the displacements on the (coarse) finite element scale and $\tilde{\boldsymbol{\sigma}} \in \tilde{\mathcal{T}}$ and $\tilde{\mathbf{u}} \in \tilde{\mathcal{V}}$ are the enhancement of the stresses and the displacements corresponding to the (finer) sub-grid scales. Let us also consider the corresponding test functions $\tilde{\boldsymbol{\tau}} \in \tilde{\mathcal{T}}$ and $\tilde{\mathbf{v}} \in \tilde{\mathcal{V}}$. This approximation extends the stress solution space to $\mathcal{T} \simeq \mathcal{T}_h \oplus \tilde{\mathcal{T}}$, and the displacement solution space to $\mathbf{V} \simeq \mathcal{V}_h \oplus \tilde{\mathcal{V}}$. Each particular stabilized finite element method is defined according to the way in which spaces $\tilde{\mathcal{T}}$ and $\tilde{\mathcal{V}}$ are chosen. In particular, the Galerkin method corresponds to taking $\tilde{\mathcal{T}} = \{\mathbf{0}\}$, $\tilde{\mathcal{V}} = \{\mathbf{0}\}$.

As it has been mentioned, in what follows we will consider continuous finite element interpolations. Likewise, we will assume that the subscales vanish on the interelement boundaries. When more general situations are considered, additional terms involving inter-element boundary integrals need to be added (see [30,42]).

Introducing the splitting, the problem corresponding to Eqs. (2a)–(2b) is:

$$-\left(\boldsymbol{\tau}_h, \mathbf{C}^{-1} : \boldsymbol{\sigma}_h\right) - \left(\boldsymbol{\tau}_h, \mathbf{C}^{-1} : \tilde{\boldsymbol{\sigma}}\right) + (\boldsymbol{\tau}_h, \nabla^s \mathbf{u}_h) - (\nabla \cdot \boldsymbol{\tau}_h, \tilde{\mathbf{u}}) = 0 \quad \forall \boldsymbol{\tau}_h \tag{5a}$$

$$-\left(\tilde{\boldsymbol{\tau}}, \mathbf{C}^{-1} : \boldsymbol{\sigma}_h\right) - \left(\tilde{\boldsymbol{\tau}}, \mathbf{C}^{-1} : \tilde{\boldsymbol{\sigma}}\right) + (\tilde{\boldsymbol{\tau}}, \nabla^s \mathbf{u}_h) + (\tilde{\boldsymbol{\tau}}, \nabla^s \tilde{\mathbf{u}}) = 0 \quad \forall \tilde{\boldsymbol{\tau}} \tag{5b}$$

$$(\nabla^s \mathbf{v}_h, \boldsymbol{\sigma}_h) + (\nabla^s \mathbf{v}_h, \tilde{\boldsymbol{\sigma}}) = \mathrm{F}(\mathbf{v}_h) \quad \forall \mathbf{v}_h \tag{5c}$$

$$-(\tilde{\mathbf{v}}, \nabla \cdot \boldsymbol{\sigma}_h) - (\tilde{\mathbf{v}}, \nabla \cdot \tilde{\boldsymbol{\sigma}}) = \mathrm{F}(\tilde{\mathbf{v}}) \quad \forall \tilde{\mathbf{v}} \tag{5d}$$

where some terms have been integrated by parts and we have assumed that $\tilde{\mathbf{u}}$ and $\tilde{\mathbf{v}}$ vanish on the boundary. In the following, the fact that the discrete variational equations need to hold for all test functions will be omitted.

Due to the approximation used, Eq. (4), and the linear independence of $\boldsymbol{\tau}_h$ and $\tilde{\boldsymbol{\tau}}$, now the continuous Eq. (2a) unfolds in two discrete Eqs. (5a) and (5b), one related to each scale considered. The same comment is applicable to the displacement splitting. Eqs. (5a) and (5c) are defined in the finite element spaces $\mathcal{T}_h$ and $\mathcal{V}_h$, respectively. The first one enforces the constitutive equation including a stabilization term $\mathbf{S}_1 = -(\boldsymbol{\tau}_h, \mathbf{C}^{-1} : \tilde{\boldsymbol{\sigma}}) - (\nabla \cdot \boldsymbol{\tau}_h, \tilde{\mathbf{u}})$ depending on the sub-grid stresses and displacements. The second one solves the balance of momentum including a stabilization term $\mathbf{S}_2 = (\nabla^s \mathbf{v}_h, \tilde{\boldsymbol{\sigma}})$ depending on the sub-grid stresses $\tilde{\boldsymbol{\sigma}}$.

Let us define the residuals of the finite element components as

$$\mathbf{r}_{\sigma,h} = \mathbf{C}^{-1} : \boldsymbol{\sigma}_h - \nabla^s \mathbf{u}_h \tag{6a}$$

$$\mathbf{r}_{u,h} = \mathbf{f} + \nabla \cdot \boldsymbol{\sigma}_h \tag{6b}$$

These allow us to write Eqs. (5b) and (5d) as

$$-\left(\tilde{\boldsymbol{\tau}}, \mathbf{C}^{-1} : \tilde{\boldsymbol{\sigma}}\right) + (\tilde{\boldsymbol{\tau}}, \nabla^s \tilde{\mathbf{u}}) = \left(\tilde{\boldsymbol{\tau}}, \mathbf{r}_{\sigma,h}\right) \tag{7a}$$

$$-(\tilde{\mathbf{v}}, \nabla \cdot \tilde{\boldsymbol{\sigma}}) = \left(\tilde{\mathbf{v}}, \mathbf{r}_{u,h}\right) \tag{7b}$$

These equations are the projections of the finite element residuals onto the space of subscales, which cannot be resolved by the finite element mesh. Therefore, to proceed it is necessary to provide an approximate closed form solution to them. If $\tilde{\mathcal{P}}_\sigma$ and $\tilde{\mathcal{P}}_u$ are the projections onto $\tilde{\mathcal{T}}$ and $\tilde{\mathcal{V}}$, respectively, note first that we may write Eqs. (7a) and (7b) as

$$\tilde{\mathcal{P}}_\sigma\left(-\mathbf{C}^{-1} : \tilde{\boldsymbol{\sigma}} + \nabla^s \tilde{\mathbf{u}}\right) = \tilde{\mathcal{P}}_\sigma\left(\mathbf{r}_{\sigma,h}\right) \tag{8a}$$

$$\tilde{\mathcal{P}}_u(-\nabla \cdot \tilde{\boldsymbol{\sigma}}) = \tilde{\mathcal{P}}_u\left(\mathbf{r}_{u,h}\right) \tag{8b}$$

and therefore the problem is to approximate the operators on the left-hand-side of these equations. The way we motivate such an approximation is by using an approximate Fourier analysis of the problem. Using exactly the same procedure as in [43], it can be shown that $\tilde{\boldsymbol{\sigma}}$ and $\tilde{\mathbf{u}}$ may be approximated *within each element* by

$$\tilde{\boldsymbol{\sigma}} = -\tau_\sigma \mathbf{C} : \tilde{\mathcal{P}}_\sigma\left(\mathbf{r}_{\sigma,h}\right) = \tau_\sigma \tilde{\mathcal{P}}_\sigma(\mathbf{C} : \nabla^s \mathbf{u}_h - \boldsymbol{\sigma}_h) \tag{9a}$$

$$\tilde{\mathbf{u}} = \tau_u \tilde{\mathcal{P}}_u\left(\mathbf{r}_{u,h}\right) = \tau_u \tilde{\mathcal{P}}_u(\mathbf{f} + \nabla \cdot \boldsymbol{\sigma}_h) \tag{9b}$$

where the so called *stabilization parameters* τ_σ and τ_u can be computed as

$$\tau_\sigma = c_\sigma \frac{h}{L_0}, \quad \tau_u = c_u \frac{L_0 h}{C_{\min}} \tag{10}$$

and where c_σ and c_u are algorithmic constants, L_0 is a characteristic length of the computational domain, h is the element size and $C_{\min} > 0$ is the smallest eigenvalue of $\mathbf{C}$ (see below). As shown in Ref. [30], this is the choice of the parameters that yields best order of convergence *for equal order of interpolation* of stresses and displacements. In the following, and for the sake of clarity, we will consider the mesh quasi-

uniform, so that a unique h can be defined for all the mesh, and thus τ_σ and τ_u will be constant. In general situations, it is understood that these parameters have to be evaluated element-wise.

The methods we wish to consider are completely defined up to the choice of the projections $\tilde{\mathcal{P}}_\sigma$ and $\tilde{\mathcal{P}}_u$. Two possible options are described next.

2.3.2. Residual-based algebraic sub-grid scale method

The simplest choice is to take $\tilde{\mathcal{P}}_\sigma$ and $\tilde{\mathcal{P}}_u$ as the identity when applied to the residuals in Eqs. (9a) and (9b). In fact, one may also think that the projection is scaled by the stabilization parameters given by Eq. (10), which act as upscaling of the residuals onto the finite element mesh. This is what is called *algebraic sub-grid scale* (ASGS) method in [30], for example. If the subscales resulting from these equations are then inserted into Eqs. (5a) and (5c) one gets

$$-(1-\tau_\sigma)\left(\boldsymbol{\tau}_h, \mathbf{C}^{-1}:\boldsymbol{\sigma}_h\right) + (1-\tau_\sigma)(\boldsymbol{\tau}_h, \nabla^s\mathbf{u}_h) - \tau_u(\nabla\cdot\boldsymbol{\tau}_h, \nabla\cdot\boldsymbol{\sigma}_h) = \tau_u(\nabla\cdot\boldsymbol{\tau}_h, \mathbf{f}) \tag{11a}$$

$$(1-\tau_\sigma)(\nabla^s\mathbf{v}_h, \boldsymbol{\sigma}_h) + \tau_\sigma(\nabla^s\mathbf{v}_h, \mathbf{C}:\nabla^s\mathbf{u}_h) = \mathrm{F}(\mathbf{v}_h) \tag{11b}$$

Note that the resulting system of equations is *symmetric*.

Particularly interesting is the case $\tau_u = 0$. In this situation, Eq. (11a) represents a projection onto the discrete finite element space that can be written as

$$\boldsymbol{\sigma}_h = P_h(\mathbf{C}:\nabla^s\mathbf{u}_h) \tag{12}$$

and, therefore, the discrete balance Eq. (11b) takes the form:

$$(1-\tau_\sigma)(\nabla^s\mathbf{v}_h, P_h(\mathbf{C}:\nabla^s\mathbf{u}_h)) + \tau_\sigma(\nabla^s\mathbf{v}_h, C:\nabla^s\mathbf{u}_h) = (\mathbf{v}_h, \mathbf{f})$$

Thus, for $\tau_u = 0$ the method we propose can be rewritten as

$$\boldsymbol{\sigma}_{\mathrm{stab}} = (1-\tau_\sigma)P_h(\mathbf{C}:\nabla^s\mathbf{u}_h) + \tau_\sigma(\mathbf{C}:\nabla^s\mathbf{u}_h) \tag{13a}$$

$$(\nabla^s\mathbf{v}_h, \boldsymbol{\sigma}_{\mathrm{stab}}) = \mathrm{F}(\mathbf{v}_h) \tag{13b}$$

This compact form of writing the problem is only possible when $\tau_u = 0$. Otherwise, Eqs. (11a)–(11b) have to be kept as such.

Some remarks are in order:

1. The stabilization term $\mathbf{S}_2$ in Eq. (5a) is computed in an element by element manner and within each element. Its magnitude depends on the difference between the continuous (projected) stresses $\boldsymbol{\sigma}_h$ and the discontinuous (elemental) stresses $\mathbf{C}$: $\nabla^s\mathbf{u}_h$.
2. This means that the term added to secure a stable solution decreases upon mesh refinement, as the finite element scale becomes finer and the *residual* reduces.
3. In other words, $\tilde{\boldsymbol{\sigma}}$ is "small" compared to $\boldsymbol{\sigma}_h$.
4. With this definition, $\tilde{\boldsymbol{\sigma}}$ is discontinuous across element boundaries. For linear elements, $\tilde{\boldsymbol{\sigma}}$ is piece-wise linear.
5. Even if defined element-wise, $\tilde{\boldsymbol{\sigma}}$ cannot be condensed at the element level, because $\boldsymbol{\sigma}_h$ is interelement continuous.
6. In the localization process in Eq. (9a), it is necessary to neglect the integrals over element faces involving the subscale, in front of the integrals over the element volumes. This is justified in [44] resorting to Fourier analysis and recalling that the subscale is associated to frequencies higher than the grid scale. It is worth to mention that for "bubble"-type enhancements these boundary terms are null by construction [45,46]. See also [42] for a possible generalization.
7. Eq. (9a) must not be interpreted *point-wise*, as the values of $\tilde{\boldsymbol{\sigma}}$ are not used in the stabilization procedure; only the integrals $\mathbf{S}_1$ and $\mathbf{S}_2$ in Eqs. (5a)–(5c) are needed.

2.3.3. Orthogonal subscale stabilization

It was argued in [27] that a very *natural* choice for the unknown sub-grid spaces is to take them orthogonal to the finite element space. This amounts to saying that the projections $\tilde{\mathcal{P}}_\sigma$ and $\tilde{\mathcal{P}}_u$ are taken as $P_h^\perp$ applied to the appropriate space of discrete functions. This also means approximating the stress solution space as $\mathcal{T} \simeq \mathcal{T}_h \oplus \mathcal{T}_h^\perp$ and, similarly, the displacement solution space as $\mathcal{V} \simeq \mathcal{V}_h \oplus \mathcal{V}_h^\perp$. The subsequent stabilization method is called *orthogonal subscale stabilization* (OSS) method, and it has already been successfully applied to several problems in fluid and solid mechanics.

Noting that $\boldsymbol{\sigma}_h$ is a finite element function and computing $P_h^\perp = I - P_h$ (I being the identity), the subscales can be now expressed as

$$\tilde{\boldsymbol{\sigma}} = \tau_\sigma P_h^\perp(\mathbf{C}:\nabla^s\mathbf{u}_h) = \tau_\sigma[\mathbf{C}:\nabla^s\mathbf{u}_h - P_h(\mathbf{C}:\nabla^s\mathbf{u}_h)] \tag{14a}$$

$$\tilde{\mathbf{u}} = \tau_u P_h^\perp(\mathbf{f} + \nabla\cdot\boldsymbol{\sigma}_h) = \tau_u[\mathbf{f} + \nabla\cdot\boldsymbol{\sigma}_h - P_h(\mathbf{f} + \nabla\cdot\boldsymbol{\sigma}_h)] \tag{14b}$$

Introducing these orthogonal subscales in Eqs. (5a) and (5c) the first component in the stabilization term $\mathbf{S}_1$ vanishes because of orthogonality and the mixed system of equations can be written as

$$-\left(\boldsymbol{\tau}_h, \mathbf{C}^{-1}:\boldsymbol{\sigma}_h\right) + (\boldsymbol{\tau}_h, \nabla^s\mathbf{u}_h) - \tau_u\left(\nabla\cdot\boldsymbol{\tau}_h, P_h^\perp(\nabla\cdot\boldsymbol{\sigma}_h)\right) = \tau_u\left(\nabla\cdot\boldsymbol{\tau}_h, P_h^\perp(\mathbf{f})\right) \tag{15a}$$

$$(\nabla^s\mathbf{v}_h, \boldsymbol{\sigma}_h) + \tau_\sigma\left(\nabla^s\mathbf{v}_h, P_h^\perp(\mathbf{C}:\nabla^s\mathbf{u}_h)\right) = \mathrm{F}(\mathbf{v}_h) \tag{15b}$$

It is also interesting to consider the case $\tau_u = 0$. Now Eq. (15a) is identical to Eq. (11a) in the previous section and, therefore, it can be written as Eq. (12) once again. With this definition, the orthogonal subscale in Eq. (14a) is identical to the residual-based subscale in Eq. (9a) with $\tilde{\mathcal{P}}_\sigma = I$. Therefore, the resulting stabilization terms are also identical and the system of Eqs. (15a)–(15b) can be arranged as in system Eqs. (11a)–(11b) or system (13a) and (13b). Therefore, when $\tau_u = 0$ the ASGS and the OSS formulations coincide.

2.4. Stability and convergence results

In this section we state stability and convergence results both for the OSS method given by Eqs. (15a)–(15b) and for the ASGS method given by Eqs. (11a)–(11b), which, as we have seen, coincide when $\tau_u = 0$. The proof of these results can be done adapting the analysis presented in [30]. To simplify the exposition, we will consider the boundary tractions $\bar{\mathbf{t}} = 0$.

The constitutive tensor $\mathbf{C}$ is assumed to be constant, symmetric and positive definite. Let $C_{\max} > 0$ and $C_{\min} > 0$ be such that

$$C_{\min}\boldsymbol{\gamma}:\boldsymbol{\gamma} \le \boldsymbol{\gamma}:\mathbf{C}:\boldsymbol{\gamma} \le C_{\max}\boldsymbol{\gamma}:\boldsymbol{\gamma} \tag{16}$$

for all symmetric second order tensors $\boldsymbol{\gamma}$.

Let $\|\cdot\|$ denote the standard norm in $L^2(\Omega)$. For the continuous problem Eqs. (2a)–(2b) it can be shown that

$$\frac{1}{C_{\max}}\|\boldsymbol{\sigma}\|^2 + \frac{L_0^h}{C_{\max}}\|\nabla\cdot\boldsymbol{\sigma}\|^2 + \frac{C_{\min}}{L_0^2}\|\mathbf{u}\|^2 + C_{\min}\|\nabla^s\mathbf{u}\|^2 \lesssim \frac{L_0^2}{C_{\min}}\|\mathbf{f}\|^2 \tag{17}$$

This result gives optimal stability in all the fields involved in the problem. The symbol $\lesssim$ is used to include constants independent of the unknowns and the components of $\mathbf{C}$ (and of h, in what follows).

For the Galerkin finite element approximation to the problem, a bound similar to Eq. (17) can be proved *provided the appropriate inf-sup conditions between the interpolating spaces are met*. Moreover, in general it is not possible to bound *both* $\|\nabla\cdot\boldsymbol{\sigma}_h\|^2$ and $\|\nabla^s\mathbf{u}_h\|^2$, but only one of these two terms.

Stabilized finite element methods aim precisely at providing stability estimates without relying on compatibility conditions. In

particular, for the methods given by Eqs. (11a)–(11b) and by Eqs. (15a)–(15b) it can be shown that

$$\frac{1}{C_{\max}}\|\boldsymbol{\sigma}_h\|^2+\frac{L_0 h}{C_{\max}}\|\nabla\cdot\boldsymbol{\sigma}_h\|^2+\frac{C_{\min}}{L_0^2}\|\mathbf{u}_h\|^2+\frac{C_{\min}h}{L_0}\|\nabla^s\mathbf{u}_h\|^2\lesssim\frac{L_0^2}{C_{\min}}\|\mathbf{f}\|^2 \tag{18}$$

where the divergence of the stresses in the left-hand-side has to be dropped if $\tau_u=0$. This estimate resembles very much Eq. (17) for the continuous problem. The only difference is the factor h instead of L_0 in two terms of the left-hand-side. This however does not prevent from obtaining the error estimates

$$\begin{aligned}&\frac{1}{C_{\max}}\|\boldsymbol{\sigma}-\boldsymbol{\sigma}_h\|^2+\frac{L_0 h}{C_{\max}}\|\nabla\cdot(\boldsymbol{\sigma}-\boldsymbol{\sigma}_h)\|^2+\\&+\frac{C_{\min}}{L_0^2}\|\mathbf{u}-\mathbf{u}_h\|^2+\frac{C_{\min}h}{L_0}\|\nabla^s(\mathbf{u}-\mathbf{u}_h)\|^2\\&\lesssim\frac{L_0}{C_{\min}}h^{2k+1}|\boldsymbol{\sigma}|_{k+1}^2+\frac{C_{\max}}{L_0}h^{2k+1}|\mathbf{u}|_{k+1}^2\end{aligned} \tag{19}$$

when interpolations of degree k are used for both the stresses and the displacements.

The symbol $|\cdot|_{k+1}$ denotes the $L^2(\Omega)$ norm of the derivatives of order $k+1$ of the unknowns, which have been assumed sufficiently regular.

The $L^2(\Omega)$ estimates given in Eq. (19) can be improved using duality arguments. The analysis in [30] can be adapted to obtain

$$\|\boldsymbol{\sigma}-\boldsymbol{\sigma}_h\|\lesssim h\|\nabla\cdot(\boldsymbol{\sigma}-\boldsymbol{\sigma}_h)\|+C_{\max}\frac{h}{L_0}\|\nabla^s(\mathbf{u}-\mathbf{u}_h)\| \tag{20}$$

$$\|\mathbf{u}-\mathbf{u}_h\|\lesssim\frac{L_0 h}{C_{\min}}\|\nabla\cdot(\boldsymbol{\sigma}-\boldsymbol{\sigma}_h)\|+h\|\nabla^s(\mathbf{u}-\mathbf{u}_h)\| \tag{21}$$

The results given by Eqs. (19)–(21) have been collected in Table 1, indicating only the order of convergence. This order is compared with what would be obtained in an irreducible formulation, where the differential equation to be solved is

$$-\nabla\cdot(\mathbf{C}:\nabla^s\mathbf{u})=\mathbf{f} \tag{22}$$

It is clear from Table 1 that the stresses are approximated with a better accuracy using the mixed stabilized formulation.

3. Nonlinear problem

3.1. Motivation

All the discussion presented heretofore is restricted to the mixed stabilized formulation of the linear elasticity problem. In this work we are interested in nonlinear constitutive behavior of materials of the form

$$\mathbf{C}=\mathbf{C}(\boldsymbol{\sigma})\quad\text{or}\quad\mathbf{C}=\mathbf{C}(\varepsilon),\quad\varepsilon=\nabla^s\mathbf{u} \tag{23}$$

which in particular can be used to model damage. Note that plasticity-type models do not fall within this framework, because in that case the constitutive equation is written in rate form. To extend the present formulation to such models will be the subject of future research.

The misbehavior encountered when irreducible formulations are used is well known, and has been described already in Section 1. The numerical problems found can be attributed to poor stability and/or accuracy in the computation of the stresses. Since they are used to evaluate the constitutive law (Eq. (23)), it is not surprising that a failure in calculating the stresses leads to a global failure of the overall numerical approximation.

Our proposal in this work is simple: numerical instabilities present in nonlinear solid mechanics using the irreducible formulation (i.e., approximating Eq. (22)) could be at least alleviated if stability and/or accuracy in the calculation of the stresses are improved. And this improvement can be achieved by using a mixed formulation. However, the price to be paid is to use interpolations for the stresses and the displacements that satisfy the inf-sup compatibility condition, and this very often leads to non-standard (if not directly exotic) interpolating pairs. The tool to overcome this is to resort to stabilized formulations, as we have shown so far.

Even though we do not have the analysis for nonlinear problems, the results presented in Section 4 suggest that success is possible. In particular:

- *Stress stability is improved*. From estimate Eq. (18) it is observed that in the linear case stress stability is obtained without relying on the stability obtained for the displacement field.
- *Stress accuracy is improved*, as it is clearly seen from Table 1 in linear elasticity. As a particular case, consider $k=1$ (linear interpolation). In the irreducible formulation the stresses are approximated with order h *in the* $L^2(\Omega)$ *norm*. Without additional conditions on the regularity of the solution and the shape of the elements of the finite element mesh, point-wise estimates are expected to have one order less of convergence. This means that *no convergence order* can be guaranteed for the stresses that are used to evaluate the constitutive law (Eq. (23)) point-wise. For the mixed stabilized formulation we can formally expect order h convergence in the worst situation (order $h^{1/2}$ if the assumptions of duality arguments do not apply).

In the following we describe how to formulate mixed stabilized methods in the nonlinear case. The first point to keep in mind is that results will be different depending on whether stresses or strains are used as independent variables to be interpolated. In the linear case there is obviously no difference, since for constant constitutive tensors $\mathbf{C}$ the space for the discrete strains $\varepsilon_h=\mathbf{C}^{-1}:\boldsymbol{\sigma}_h$ is the same as the space for the discrete stresses σ_h, and formulating the mixed methods presented in Section 2.4 in strains is trivial.

3.2. Stress/displacement formulation

For the sake of conciseness, in this subsection we assume that $\tilde{\mathbf{u}}=\mathbf{0}$. Including displacement subscales in the following discussion is straightforward. The only remarks to be made are that the ASGS and the OSS methods will not yield the same methods, as we have seen, and stability and convergence for the divergence of the stresses will be lost if $\tilde{\mathbf{u}}=\mathbf{0}$.

3.2.1. General formulation

Introducing the scale splitting as described in Subsection 2.3.1 we arrive at problem Eq. (5a)–Eq. (5d) also in the nonlinear case. In the case $\tilde{\mathbf{u}}=\mathbf{0}$, we may rewrite this problem as

$$-\left(\boldsymbol{\tau}_h,\mathbf{C}^{-1}:\boldsymbol{\sigma}_h\right)-\left(\boldsymbol{\tau}_h,\mathbf{C}^{-1}:\tilde{\boldsymbol{\sigma}}\right)+\left(\boldsymbol{\tau}_h,\nabla^s\mathbf{u}_h\right)=0 \tag{24a}$$

$$\left(\nabla^s\mathbf{v}_h,\boldsymbol{\sigma}_h\right)+\left(\nabla^s\mathbf{v}_h,\tilde{\boldsymbol{\sigma}}\right)=\left(\mathbf{v}_h,\mathbf{f}\right) \tag{24b}$$

$$-\tilde{\mathcal{P}}_\sigma\left(\mathbf{C}^{-1}:\tilde{\boldsymbol{\sigma}}\right)=\tilde{\mathcal{P}}_\sigma\left(\mathbf{C}^{-1}:\boldsymbol{\sigma}_h\right)-\tilde{\mathcal{P}}_\sigma\left(\nabla^s\mathbf{u}_h\right) \tag{24c}$$

Table 1
Order of convergence of different terms in the irreducible and mixed stabilized formulations when interpolations of degree k are used.

Term	Irreducible	Mixed
$\|\nabla^s(\mathbf{u}-\mathbf{u}_h)\|$	h^k	h^k
$\|\mathbf{u}-\mathbf{u}_h\|$	h^{k+1} with duality	$h^{k+1/2}$ without duality, h^{k+1} with duality
$\|\boldsymbol{\sigma}-\boldsymbol{\sigma}_h\|$	h^k ($\boldsymbol{\sigma}_h=\mathbf{C}:\nabla^s\mathbf{u}_h$)	$h^{k+1/2}$ without duality, h^{k+1} with duality
$\|\nabla\cdot(\boldsymbol{\sigma}-\boldsymbol{\sigma}_h)\|$	h^{k-1} ($\boldsymbol{\sigma}_h=\mathbf{C}:\nabla\mathbf{u}_h$)	h^k (if $c_u>0$ in Eq. (10))

where Eq. (24c) corresponds to Eq. (8a). Let us see how to particularize this general framework to the ASGS and the OSS methods.

3.2.1.1. ASGS method. In this case $\tilde{\mathcal{P}}_\sigma = I$ when applied to the residual scaled by τ_σ, and we may approximate

$$\tilde{\boldsymbol{\sigma}} = \tau_\sigma(\mathbf{C} : \nabla^s \mathbf{u}_h - \boldsymbol{\sigma}_h) \tag{25}$$

Note that if $\tau_\sigma \neq 1$ then $\tilde{\boldsymbol{\sigma}} + \boldsymbol{\sigma}_h \neq \mathbf{C}:\nabla^s \mathbf{u}_h$. As it has been mentioned previously, the scaling of the residual by τ_σ can be understood as the upscaling of $\tilde{\boldsymbol{\sigma}}$ to the finite element mesh.

From Eqs. (24a)–(25) it follows that Eqs. (11a)–(11b) are still valid in the nonlinear case, that is to say,

$$-\left(\boldsymbol{\tau}_h, \mathbf{C}^{-1} : \boldsymbol{\sigma}_h\right) + (\boldsymbol{\tau}_h, \nabla^s \mathbf{u}_h) = 0 \tag{26a}$$

$$(1-\tau_\sigma)(\nabla^s \mathbf{v}_h, \boldsymbol{\sigma}_h) + \tau_\sigma(\nabla^s \mathbf{v}_h, \mathbf{C} : \nabla \mathbf{u}_h) = (\mathbf{v}_h, \mathbf{f}) \tag{26b}$$

Even though the discrete problem is already given by Eqs. (26a)–(26b), it is suggestive to write it in a form similar to Eqs. (13a)–(13b). Let $P_{C^{-1}}$ denote the $L^2(\Omega)$ projection onto the finite element space of stresses *weighted by* $\mathbf{C}^{-1}$. Since $(\boldsymbol{\tau}_h, \nabla^s \mathbf{u}_h) = (\tau_h, \mathbf{C}^{-1}:\mathbf{C}:\nabla^s \mathbf{u}_h)$, we may write Eq. (26a) as

$$\boldsymbol{\sigma}_h = P_{C^{-1}}(\mathbf{C} : \nabla^s \mathbf{u}_h) \tag{27}$$

from where it follows that, similar to Eqs. (13a)–(13b), the ASGS formulation can be expressed as

$$\boldsymbol{\sigma}_{\text{stab}} = (1-\tau_\sigma) P_{C^{-1}}(\mathbf{C} : \nabla^s \mathbf{u}_h) + \tau_\sigma(\mathbf{C} : \nabla^s \mathbf{u}_h) \tag{28a}$$

$$(\nabla^s \mathbf{v}_h, \boldsymbol{\sigma}_{\text{stab}}) = \mathrm{F}(\mathbf{v}_h) \tag{28b}$$

Clearly, for constant constitutive tensors $\mathbf{C}$ there is no difference between Eqs. (28a)–(28b) and (13a)–(13b), but the weighted $L^2(\Omega)$ projection should be in principle taken into account in nonlinear constitutive models or simply when the medium is not homogeneous.

3.2.1.2. OSS method. The first option would be to take $\tilde{\mathcal{P}}_\sigma = P_h^\perp$. In this case, Eq. (24c) becomes

$$-P_h^\perp\left(\mathbf{C}^{-1} : \tilde{\boldsymbol{\sigma}}\right) = P_h^\perp\left(\mathbf{C}^{-1} : \boldsymbol{\sigma}_h\right) - P_h^\perp(\nabla^s \mathbf{u}_h) \tag{29}$$

However, it is not computationally simple to obtain an expression for the sub-grid stresses from this equation. To construct a basis for the orthogonal to the space of stresses is required to invert the left-hand-side. A simpler and perhaps more natural option is to take $\tilde{\mathcal{T}}$ orthogonal to $\mathcal{T}_h$ *with respect to* $P_{C^{-1}}$. From Eq. (24c) it immediately follows that

$$\tilde{\boldsymbol{\sigma}} = \tau_\sigma P_{C^{-1}}^\perp(\mathbf{C} : \nabla^s \mathbf{u}_h) \tag{30}$$

and, as for the linear elasticity problem, it can be shown that the OSS and the ASGS formulations coincide and are given by Eqs. (28a)–(28b).

3.2.2. Simplifications

System (28a)–(28b) can be approximated as is, but there are two approximations that simplify its numerical implementation:

- $\mathbf{C}(\boldsymbol{\sigma}) \approx \mathbf{C}(\boldsymbol{\sigma}_h)$. Even though we have not explicitly indicated it earlier, the dependence of $\mathbf{C}$ on the stresses needs to be approximated. One possibility is to use $\boldsymbol{\sigma}_{\text{stab}}$ given by Eqs. (28a)–(28b), although, since the subscales are expected to be much smaller than the finite element scales, $\mathbf{C}$ can be evaluated also with $\boldsymbol{\sigma}_h$. This simplifies the implementation when the displacement subscales are accounted for (see Eqs. (11a)–(11b)).
- $P_{C^{-1}} \approx P_h$. At the computational level, it is much easier to deal with the standard $L^2(\Omega)$ projection than with the weighted one. In particular, simpler numerical integration rules may be used. Likewise, lumping of the matrix resulting from the projection is possible.

3.3. Strain/displacement formulation

3.3.1. General formulation

The formulation of the mixed solid mechanics problem in terms of the stress and displacement fields, $\boldsymbol{\sigma}/\mathbf{u}$, is classical and it has been used many times in the context of *linear elasticity*, where the constitutive tensor $\mathbf{C}$ is constant. However, it is not the most convenient format for the nonlinear problem. The reason for this is that most of the algorithms used for nonlinear constitutive equations in solid mechanics have been derived for the irreducible formulation. This means that these procedures are usually *strain driven,* and they have a format in which the stress $\boldsymbol{\sigma}$ is computed in terms of the strain $\boldsymbol{\varepsilon}$, with $\boldsymbol{\varepsilon} = \nabla^s \mathbf{u}$.

Therefore, in order to be able to use the existing technology available for the integration of nonlinear constitutive equations, it is convenient to derive a mixed strain/displacement, $\boldsymbol{\varepsilon}/\mathbf{u}$, stabilized formulation for the nonlinear solid mechanics problem. In view of the previous developments this is easily accomplished.

In this case, the strong form of the continuous problem can be stated as: for given prescribed body forces $\mathbf{f}$, find the displacement field $\mathbf{u}$ and the strain field $\boldsymbol{\varepsilon}$ such that:

$$-\mathbf{C} : \boldsymbol{\varepsilon} + \mathbf{C} : \nabla^s \mathbf{u} = \mathbf{0} \qquad \text{in } \Omega \tag{31a}$$

$$\nabla\cdot(\mathbf{C} : \boldsymbol{\varepsilon}) + \mathbf{f} = \mathbf{0} \qquad \text{in } \Omega \tag{31b}$$

Eq. (31a) represents strain compatibility, while Eq. (31b) is the Cauchy equation. Eqs. (31a)–(31b) are subjected to appropriate Dirichlet and Neumann boundary conditions.

If $\mathcal{V}$ is, as before, the space of displacements and $\mathcal{G}$ the space of strains, following the standard procedure the associated weak form of the problem Eqs. (31a)–(31b) can be stated as:

$$-(\boldsymbol{\gamma}, \mathbf{C} : \boldsymbol{\varepsilon}) + (\boldsymbol{\gamma}, \mathbf{C} : \nabla^s \mathbf{u}) = 0 \qquad \forall \boldsymbol{\gamma} \tag{32a}$$

$$(\nabla^s \mathbf{v}, \mathbf{C} : \boldsymbol{\varepsilon}) = (\mathbf{v}, \mathbf{f}) \qquad \forall \mathbf{v} \tag{32b}$$

where $\mathbf{v} \in \mathcal{V}$ and $\boldsymbol{\gamma} \in \mathcal{G}$ are the test functions of the displacements and strain fields, respectively. Eqs. (31a)–(31b) can be understood as the stationary conditions of the classical (reduced) Hu–Washizu functional [41].The *discrete Galerkin* finite element counterpart problem is:

$$-(\boldsymbol{\gamma}_h, \mathbf{C} : \boldsymbol{\varepsilon}_h) + (\boldsymbol{\gamma}_h, \mathbf{C} : \nabla^s \mathbf{u}_h) = 0 \qquad \forall \boldsymbol{\gamma}_h \tag{33a}$$

$$(\nabla^s \mathbf{v}_h, \mathbf{C} : \boldsymbol{\varepsilon}_h) = \mathrm{F}(\mathbf{v}_h) \qquad \forall \mathbf{v}_h \tag{33b}$$

where $\mathbf{u}_h$, $\mathbf{v}_h \in \mathcal{V}_h$ and $\boldsymbol{\varepsilon}_h, \Upsilon_h \in \mathcal{G}_h$ are the *discrete* displacement and strain fields and their test functions, defined onto the finite element spaces $\mathcal{V}_h$ and $\mathcal{G}_h$, respectively. Note that the resulting system of equations is *symmetric* but *non-definite*.

Stability considerations for the mixed $\boldsymbol{\varepsilon}/\mathbf{u}$ are analogous to those of the $\boldsymbol{\sigma}/\mathbf{u}$ format, so we proceed to present a stabilization method, using the residual-based sub-grid scale approach, which allows in particular the use of linear/linear interpolations for displacements and strains. To this end, the strain field of the mixed problem is approximated as

$$\boldsymbol{\varepsilon} = \boldsymbol{\varepsilon}_h + \tilde{\boldsymbol{\varepsilon}} \tag{34}$$

where $\boldsymbol{\varepsilon}_h \in \mathcal{G}_h$ is the strain component of the (coarse) finite element scale and $\tilde{\boldsymbol{\varepsilon}} \in \tilde{\mathcal{G}}$ is the enhancement of the strain field corresponding to the (finer) sub-grid scale. Let us also consider the corresponding test functions $\boldsymbol{\gamma}_h \in \mathcal{G}_h$ and $\tilde{\boldsymbol{\gamma}} \in \tilde{\mathcal{G}}$, respectively. The strain solution space is

$\mathcal{G} \simeq \mathcal{G}_h \oplus \tilde{\mathcal{G}}$. For simplicity, no subscale will be considered for the displacement field for the moment. Its inclusion is considered in Subsection 3.4. Thus, considering only the strain subscale, the discrete problem corresponding to Eqs. (32a) and (32b) is now:

$$-(\gamma_h, \mathbf{C} : \varepsilon_h) - (\gamma_h, \mathbf{C} : \tilde{\varepsilon}) + (\gamma_h, \mathbf{C} : \nabla^s \mathbf{u}_h) = 0 \qquad \forall \gamma_h \tag{35a}$$

$$-(\tilde{\gamma}, \mathbf{C} : \varepsilon_h) - (\tilde{\gamma}, \mathbf{C} : \tilde{\varepsilon}) + (\tilde{\gamma}, \mathbf{C} : \nabla^s \mathbf{u}_h) = 0 \qquad \forall \tilde{\gamma} \tag{35b}$$

$$(\nabla^s \mathbf{v}_h, \mathbf{C} : \varepsilon_h) + (\nabla^s v_h, \mathbf{C} : \tilde{\varepsilon}) = \mathrm{F}(\mathbf{v}_h) \quad \forall \mathbf{v}_h \tag{35c}$$

As for the stress–displacement approach, the fact that the discrete variational equations need to hold for all test functions will be omitted in the following.

Due to the approximation used in Eq. (34), and the linear independence of $\boldsymbol{\varepsilon}_h$ and $\tilde{\boldsymbol{\varepsilon}}$, the continuous Eq. (32a) unfolds in two discrete Eqs. (35a) and (35b), one related to each scale considered. Eqs. (35a) and (35c) are defined in the finite element spaces $\mathcal{G}_h$ and $\mathcal{V}_h$, respectively. The first one enforces the constitutive equation including a stabilization term $\mathbf{S}_1 = (\boldsymbol{\gamma}_h, \mathbf{C}: \tilde{\varepsilon})$ depending on the sub-grid strains $\tilde{\varepsilon}$. The second one solves the balance of momentum including a stabilization term $\mathbf{S}_2 = (\nabla^s \mathbf{v}_h, \mathbf{C}:\tilde{\varepsilon})$ depending on the sub-grid stresses $\tilde{\boldsymbol{\sigma}} = \mathbf{C}: \tilde{\varepsilon}$. On the other hand, Eq. (35b) is defined in the sub-grid scale space $\tilde{\mathcal{G}}$ and, hence, it cannot be solved by the finite element mesh.

Following the same arguments introduced in the previous section, we can write Eq. (35b) as

$$-(\tilde{\gamma}, \mathbf{C} : \tilde{\varepsilon}) = (\tilde{\gamma}, \mathbf{r}_h) \tag{36}$$

where the residual of the constitutive equation in the finite element scale is defined as:

$$\mathbf{r}_h = \mathbf{r}_h(\varepsilon_h, \mathbf{u}_h) = \mathbf{C} : \varepsilon_h - \mathbf{C} : \nabla^s \mathbf{u}_h \tag{37}$$

In the case of the residual-based ASGS formulation, the subscale stress can be *localized* within each finite element, and be expressed as

$$\tilde{\varepsilon} = \tau_\varepsilon \mathbf{C}^{-1} : \mathbf{r}_h = \tau_\varepsilon \left[\nabla^s \mathbf{u}_h - \varepsilon_h\right] \tag{38}$$

where $\tau_{\boldsymbol{\varepsilon}}$ is computed in terms of an algorithmic constant $c_{\boldsymbol{\varepsilon}}$ as

$$\tau_\varepsilon = c_\varepsilon \frac{h}{L_0} \tag{39}$$

Introducing the strain subscale from Eq. (38) in Eq. (35a), the mixed system of equations can be written as

$$-(1-\tau_\varepsilon)(\gamma_h, \mathbf{C} : \varepsilon_h) + (1-\tau_\varepsilon)(\gamma_h, \mathbf{C} : \nabla^s \mathbf{u}_h) = 0 \tag{40a}$$

$$(1-\tau_\varepsilon)(\nabla^s \mathbf{v}_h, \mathbf{C} : \varepsilon_h) + \tau_\varepsilon(\nabla^s \mathbf{v}_h, \mathbf{C} : \nabla^s \mathbf{u}_h) = \mathrm{F}(\mathbf{v}_h) \tag{40b}$$

where the terms depending on $\tau_{\boldsymbol{\varepsilon}}$ represent the stabilization. Note that the resulting system of equations is *symmetric*.

If P_C is the $L^2(\Omega)$ projection *weighted by* $\mathbf{C}$, the projection involved in Eq. (40a) can be written as

$$\varepsilon_h = P_C(\nabla^s \mathbf{u}_h) \tag{41}$$

and, therefore, the weak form of the balance Eq. (40b), can be finally written as:

$$(1-\tau_\varepsilon)(\nabla^s \mathbf{v}_h, \mathbf{C} : P_C(\nabla^s \mathbf{u}_h)) + \tau_\varepsilon(\nabla^s \mathbf{v}_h, \mathbf{C} : \nabla^s \mathbf{u}_h) = \mathrm{F}(\mathbf{v}_h) \tag{42}$$

Eq. (38) does not need to be interpreted *point-wise*, as the values of $\tilde{\varepsilon}$ are not used in the stabilization procedure; only the integral S_2 in Eq. (35c) is needed.

Similar to the stress–displacement formulation Eqs. (28a)–(28b), we can finally write the method we propose for the strain–displacement approach as

$$\varepsilon_{\mathrm{stab}} = (1-\tau_\varepsilon) P_C(\nabla^s \mathbf{u}_h) + \tau_\varepsilon(\nabla^s \mathbf{u}_h) \tag{43a}$$

$$(\nabla^s \mathbf{v}_h, \mathbf{C} : \boldsymbol{\varepsilon}_{\mathrm{stab}}) = \mathbf{F}(\mathbf{v}_h) \tag{43b}$$

This approach is of straightforward implementation.

As in the previous section, some remarks are relevant:

1. The stabilization term $\mathbf{S}_2$ is computed in an element by element manner and, within each element, its magnitude depends on the difference between the continuous (projected) and the discontinuous (elemental) strain fields. This means that the term added to secure a stable solution decreases upon mesh refinement, as the finite element scale becomes finer and the *residual* (or the *projection of the residual)* reduces ($\tilde{\boldsymbol{\varepsilon}}$ is "small" compared to $\boldsymbol{\varepsilon}_h$).
2. With the definition in Eq. (38), the subscale $\tilde{\varepsilon}$ is discontinuous across element boundaries. For linear elements, $\tilde{\varepsilon}$ is piece-wise linear. Therefore, even if defined element-wise, $\tilde{\varepsilon}$ cannot be condensed at element level, because $\boldsymbol{\varepsilon}_h$ is interelement continuous.

The OSS formulation can be developed using the same reasoning as for the stress–displacement approach. In this case, it is easy to show that if the strain subscale is taken orthogonal to the finite element space with respect to the $L^2(\Omega)$ inner product weighted by $\mathbf{C}$, the resulting formulation is identical to the ASGS method. Details of the derivation are omitted.

3.3.2. Simplifications

Analogously to the stress–displacement formulation, system Eqs. (43a)–(43b) can be approximated as is, but there are two approximations that simplify the implementation:

- $\mathbf{C}(\varepsilon) \approx \mathbf{C}(\varepsilon_h)$.
- $P_C \approx P_h$

The same remarks as for the stress–displacement formulation are applicable to these approximations.

3.4. Comparison between the $\boldsymbol{\sigma}/\mathbf{u}$ and the $\boldsymbol{\varepsilon}/\mathbf{u}$ formulations and final numerical schemes

As it has been mentioned, the stress–displacement and the strain–displacement formulations will lead to (slightly) different results in the nonlinear case. If we assume in both cases that $\boldsymbol{\sigma}_h = \mathbf{C}:\boldsymbol{\varepsilon}_h$, we have obtained

$$\text{Stress} - \text{displacement}: \quad \boldsymbol{\sigma}_h = P_{C^{-1}}(\mathbf{C} : \nabla \mathbf{u}_h), \quad \varepsilon_h = \mathbf{C}^{-1} : P_{C^{-1}}(\mathbf{C} : \nabla \mathbf{u}_h)$$

$$\text{Strain} - \text{displacement}: \quad \boldsymbol{\sigma}_h = \mathbf{C} : P_C(\nabla \mathbf{u}_h), \quad \varepsilon_h = P_C(\nabla \mathbf{u}_h)$$

and for the simplified formulations:

$$\text{Stress} - \text{displacement}: \quad \boldsymbol{\sigma}_h = P_h(\mathbf{C} : \nabla \mathbf{u}_h), \quad \varepsilon_h = \mathbf{C}^{-1} : P_h(\mathbf{C} : \nabla \mathrm{u}_h)$$

$$\text{Strain} - \text{displacement}: \quad \boldsymbol{\sigma}_h = \mathbf{C} : P_h(\nabla \mathbf{u}_h), \quad \varepsilon_h = P_h(\nabla u_h)$$

It is observed that only when $\mathbf{C}$ is constant both formulations coincide.

For completeness, let us finally state the expression of the $\boldsymbol{\sigma}/\mathbf{u}$ and $\boldsymbol{\varepsilon}/\mathbf{u}$ mixed forms:

$$\text{Stress} - \text{displacement}: \tag{44a}$$

$$-\left(\boldsymbol{\tau}_h, \mathbf{C}^{-1} : \boldsymbol{\sigma}_h\right) - \tau_\sigma\left(\boldsymbol{\tau}_h, \mathbf{C}^{-1} : \tilde{P}_\sigma(\mathbf{C} : \nabla \mathbf{u}_h - \boldsymbol{\sigma}_h)\right)$$

$$+ (\boldsymbol{\tau}_h, \nabla^s \mathbf{u}_h) - \tau_u \left(\nabla \cdot \boldsymbol{\tau}_h, \tilde{P}_u(\nabla \cdot \boldsymbol{\sigma}_h) \right) = \tau_u \left(\nabla \cdot \boldsymbol{\tau}_h, \tilde{P}_u(\mathbf{f}) \right)$$

$$(\nabla^s \mathbf{v}_h, \boldsymbol{\sigma}_h) + \tau_\sigma \left(\nabla^s \mathbf{v}_h, \tilde{P}_\sigma(\mathbf{C} : \nabla \mathbf{u}_h - \boldsymbol{\sigma}_h) \right) = \mathrm{F}(\mathbf{v}_h) \tag{44b}$$

Strain–displacement:

$$-(\boldsymbol{\gamma}_h, \mathbf{C} : \boldsymbol{\varepsilon}_h) - \tau_\varepsilon \left(\boldsymbol{\gamma}_h, \mathbf{C} : \tilde{P}_\varepsilon(\nabla \mathbf{u}_h - \boldsymbol{\varepsilon}_h) \right) \tag{45a}$$

$$+ (\boldsymbol{\gamma}_h, \mathbf{C} : \nabla^s \mathbf{u}_h) - \tau_u \left(\nabla \cdot (\mathbf{C} : \boldsymbol{\gamma}_h), \tilde{P}_u(\nabla \cdot (\mathbf{C} : \boldsymbol{\varepsilon}_h)) \right)$$

$$= \tau_u \left(\nabla \cdot (\mathbf{C} : \boldsymbol{\gamma}_h), \tilde{P}_u(\mathbf{f}) \right)$$

$$(\nabla^s \mathbf{v}_h, \mathbf{C} : \boldsymbol{\varepsilon}_h) + \tau_\varepsilon \left(\nabla^s \mathbf{v}_h, \mathbf{C} : \tilde{P}_\varepsilon(\nabla \mathbf{u}_h - \boldsymbol{\varepsilon}_h) \right) = \mathrm{F}(\mathbf{v}_h) \tag{45b}$$

where the (simplified) projections are taken as $\tilde{P} = I$ for ASGS and $\tilde{P} = P_h^\perp$ for OSS and $\mathbf{C} = \mathbf{C}(\boldsymbol{\sigma}_h)$ or $\mathbf{C} = \mathbf{C}(\boldsymbol{\varepsilon}_h)$.

4. Implementation and computational aspects

In this section, some relevant aspects concerning the implementation of the mixed strain/displacement scale stabilized method for nonlinear solid mechanics formulated previously are described. Implementation of the mixed stress/displacement scale stabilized method follows analogous arguments.

Due to the nonlinear dependence of the stresses on the strain and displacements, the solution of the system of Eqs. (41)–(42) requires the use of an appropriate incremental/iterative procedure such as the Newton–Raphson method. Within such a procedure, the system of linear equations to be solved for the $(i+1)$-th equilibrium iteration of the $(n+1)$-th time (or load) step is:

$$\begin{bmatrix} -\mathbf{M}_\tau & \mathbf{G}_\tau \\ \mathbf{G}_\tau^T & \mathbf{K}_\tau \end{bmatrix}^{(i)} \begin{bmatrix} \delta\mathbf{E} \\ \delta\mathbf{U} \end{bmatrix}^{(i+1)} = - \begin{bmatrix} \mathbf{R}_1 \\ \mathbf{R}_2 \end{bmatrix}^{(i)} \tag{46}$$

where $\delta\mathbf{E}$ and $\delta\mathbf{U}$ are the iterative corrections to the nodal values for the strains and displacements, respectively, $\boldsymbol{R}_1$ and $\boldsymbol{R}_2$ are the residual vectors associated to the satisfaction of the kinematic and balance of momentum equations, respectively, and the global matrices $\mathbf{M}_\tau^{(i)}$, $\mathbf{G}_\tau^{(i)}$ and $\mathbf{K}_\tau^{(i)}$ come from the standard assembly procedure of the elemental contributions. The global matrix is symmetric. Each one of the elemental matrices to be assembled has an entry $(\cdot)^{AB}$, a sub-matrix corresponding to the local nodes A and B. Let us assume in the following that the same interpolation functions N are used for the strain and displacement fields.

Sub-matrix $\mathbf{K}_\tau^{AB}$ is obtained from the standard tangent stiffness matrix:

$$\mathbf{K}_\tau^{AB} = \tau_\varepsilon \int_{\Omega_e} \mathbf{B}_A^T \mathbf{C}_{\tan} \mathbf{B}_B d\Omega \tag{47}$$

where $\mathbf{C}_{\tan}$ is the tangent constitutive matrix and $\mathbf{B}$ is the standard deformation sub-matrix. The generic term of the discrete symmetric gradient matrix operator $\mathbf{G}^{AB}$ is given by:

$$\mathbf{G}_\tau^{AB} = (1-\tau_\varepsilon) \int_{\Omega_e} \mathbf{B}_A^T \mathbf{C}_{\tan} \mathbf{N}_B d\Omega \tag{48}$$

Finally, $\mathbf{M}^{AB}$ is a "mass" matrix associated to the strain field:

$$\mathbf{M}_\tau^{AB} = (1-\tau_\varepsilon) \int_{\Omega_e} \mathbf{N}_A^T \mathbf{C}_{\tan} \mathbf{N}_B d\Omega + \tau_u \int_{\Omega_e} \hat{\mathbf{B}}_A^T \hat{\mathbf{B}}_B d\Omega \tag{49}$$

where $\hat{\mathbf{B}}_A$ is the matrix arising from applying the divergence operator to the matrix product $\mathbf{C}_{\tan}\mathbf{N}_A$.

When considering the efficient solution of system (Eq. (46)) three remarks have to be made:

- The monolithic solution of Eq. (46) can be substituted by an iterative procedure, such as

$$-\mathbf{M}_\tau^{(i)} \delta\mathbf{E}^{(i+1)} = -\boldsymbol{R}_1^{(i)} - \left[\mathbf{G}_\tau^{(i)} \right] \delta\mathbf{U}^{(i)} \tag{50a}$$

$$\mathbf{K}_\tau^{(i)} \delta\mathbf{U}^{(i+1)} = -\boldsymbol{R}_2^{(i)} - \left[\mathbf{G}_\tau^{(i)} \right]^T \delta\mathbf{E}^{(i+1)} \tag{50b}$$

- More efficient is to use an approximate staggered procedure, in which the strain projection is kept constant during the equilibrium iterations within each time increment, taking it equal to an appropriate prediction such as $\mathbf{E}^{(i+1)} \cong \mathbf{E}^{(0)}$, computed from the known values corresponding to the previous time steps (for instance, a trivial prediction consists of taking $\mathbf{E}^{(0)} \cong \mathbf{E}^{[n]}$). This scheme leads to

$$\mathbf{K}_\tau^{(i)} \delta\mathbf{U}^{(i+1)} = -\boldsymbol{R}_2 \left(\mathbf{E}^{(0)}, \mathbf{U}^{(i)} \right) \tag{51}$$

- If $\tau_u = 0$, using an appropriate integration scheme, the mass matrix $\mathbf{M}_\tau$ can be rendered block-diagonal. The resulting lumped matrix $\overline{\mathbf{M}}_\tau$ is computationally more efficient. If $\tau_u \neq 0$, this matrix $\overline{\mathbf{M}}_\tau$ is used as preconditioner of the iterative strategy.

Independently of the solution strategy adopted, it is *formally* possible to express $\mathbf{E} = [\mathbf{M}_\tau^{-1} \mathbf{G}_\tau]^{(i)} \mathbf{U}$, and substitute this value in the equilibrium equation to obtain a reduced system of equations with the form:

$$\left[\mathbf{K}_\tau + \mathbf{G}_\tau^{\mathrm{T}} \mathbf{M}_\tau^{-1} \mathbf{G}_\tau \right]^{(i)} \mathbf{U} = \mathbf{F} \tag{52}$$

where matrices $\mathbf{M}_\tau^{(i)}$, $\mathbf{G}_\tau^{(i)}$ and $\mathbf{K}_\tau^{(i)}$ are evaluated with a *secant* constitutive matrix, rather than tangent. If, as assumed in this work, the strain field $\boldsymbol{\varepsilon}_h$ is interelement continuous, the elimination of the projection $\mathbf{E}$ is not feasible in practice, because the condensation procedure cannot be performed at element level; if performed at global level it would yield a system reduced but with a spoiled banded structure. However, in this reduced format the overall effect of the proposed stabilization method becomes self-evident. It is interesting to note that it resembles the format of the enhanced assumed strain method [5] and the more general mixed-enhanced strain method [47], where the enhancing fields are discontinuous and their variables can be condensed at local level.

5. Numerical results

In this section the formulation presented above is demonstrated in two benchmark problems and an additional illustrative example. In the three cases, linear elastic constitutive behavior is assumed, with the following material properties: Young's modulus $E = 200 \cdot 10^9$ Pa, Poisson's ratio $\nu = 0.3$. Examples concerning nonlinear constitutive behavior are presented in the companion paper [40].

The first two tests are used in Ref. [5] to validate the Enhanced Assumed Strain method. Performance of the formulation is tested considering *2D plane-strain quadrilateral and triangular structured meshes*. The elements used are: *P1* (linear displacement), *P1P1* (linear strain/linear displacement), *Q1* (bilinear displacement), *Q1Q1* (bilinear strain/bilinear displacement) and *Q1E4* (bilinear displacement with enhanced strains [5]).

When the stabilized mixed strain/displacement formulation is used, values $c_{\boldsymbol{\varepsilon}} = 1.0$ and $c_u = 0.1$ are taken for the evaluation of the

stabilization parameters τ_ε and τ_u, respectively. We have chosen $C_{\min} = E$, understanding that the Young's modulus E is a characteristic value of the elastic tensor (constants appearing in the minimum eigenvalue of the elastic tensor may be included in the algorithmic constant c_u in Eq. (10)).

Calculations are performed with an enhanced version of the finite element code COMET [48], developed by the authors at the International Center for Numerical Methods in Engineering (CIMNE). Pre and post-processing is done with GiD [49], also developed at CIMNE. The stabilized system of equations resulting from the mixed method, Eq. (46) is solved both in a monolithic way and using the iterative algorithm in Eqs. (50a)–(50b).

5.1. Cook's membrane problem

The Cook membrane problem is a bending dominated example that has been used by many authors as a reference test to check their element formulations. Here it will be used to compare results for the mixed and irreducible formulations in compressible elasticity, showing the behavior of both bilinear quadrilateral and linear triangular elements.

The problem consists of a tapered panel, clamped on one side and subjected to a shearing vertical load at the free end. Geometry of this plane-strain problem is shown in Fig. 1 (dimensions are in mm). For the evaluation of the stabilization parameters in the mixed formulation, $L_0 = 50$ mm is taken as the representative length of the problem.

In order to test the convergence behavior of the different formulations, the problem has been discretized into structured meshes with N finite elements along each side. Figs. 2 and 3 compare the results obtained with five different spatial discretizations.

Fig. 2 shows the relative convergence of the five discretizations on the computed value of the vertical displacement at the right top corner of the membrane (point A in Fig. 1). Results are clearly different for the irreducible and the mixed elements and it is evident that the mixed formulation performs better for coarse and fine meshes. It also shows a slightly faster convergence rate. The performance of the mixed *Q1Q1* is very similar to the *Q1E4* quadrilateral, although the latter seems to be more accurate on very coarse meshes and slightly less accurate when the mesh is refined.

Fig. 3 shows similar results on the computed value of the major principal stress at the mid-side point of the bottom boundary of the membrane (point B in Fig. 1). It has to be noted that in order to compare stress values computed at the same point, the values reported for the irreducible and strain enhanced elements correspond to the continuous projection $P_h(\mathbf{C}:\nabla^s\mathbf{u}_h)$ evaluated at the mesh nodes, rather than the actual discontinuous stresses $\mathbf{C}:\nabla^s\mathbf{u}_h$ evaluated at the integration points. This projection procedure yields improved stress values for the irreducible formulation. Relative convergence characteristics on the stress values among the different elements compared are very similar to those observed for the displacements, and faster for the mixed and enhanced formulations than for the irreducible one.

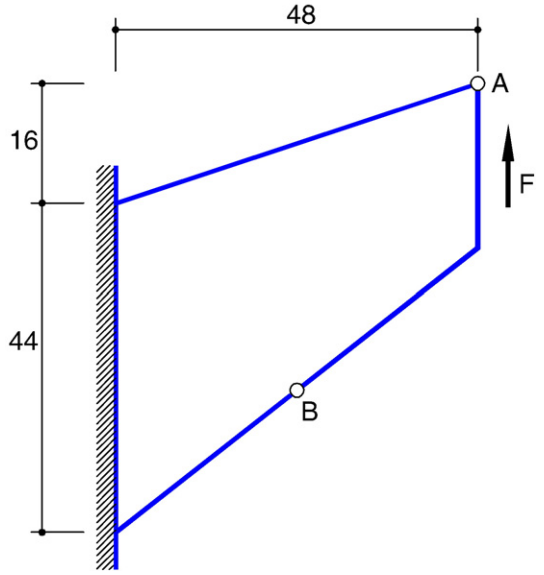

Fig. 1. Geometry for the Cook membrane problem (dimensions are in mm).

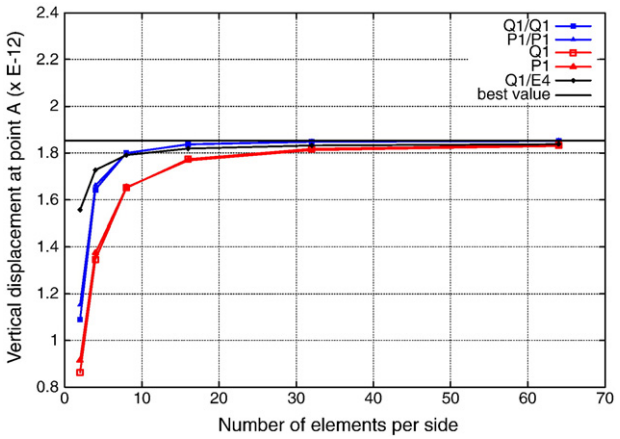

Fig. 2. Cook's membrane problem. Vertical displacement at point A versus number of elements along each side.

Regarding relative computational efficiency, Table 2 shows the CPU time used by the different formulations to solve increasingly fine quadrilateral meshes. A direct solver with skyline storage has been used in all cases. The enhanced strain formulation is only marginally more expensive than the standard one, because the size of the system of equations to be solved is identical in both cases, even if the corresponding matrices and vector are more elaborated for the first one. The efficiency of the mixed formulation depends very much on the implementation scheme adopted. On one hand, the relative cost of solving the monolithic solution of system Eq. (46), labelled *Q1Q1* (m) in the Table, grows quickly with the number of nodes in the mesh. Memory requirements for direct solvers also increase rapidly in this case. On the other hand, the iterative solution of Eqs. (50a)–(50b), labelled *Q1Q1* (i) in the Table, can be obtained at a cost that compares reasonably with those of the irreducible and enhanced strain formulations.

It has to be remarked that the relative increase in the cost of the mixed formulation with regard to the irreducible one is smaller in nonlinear problems, because iterations can be performed to solve the mixed problem and the nonlinearity in a concurrent manner.

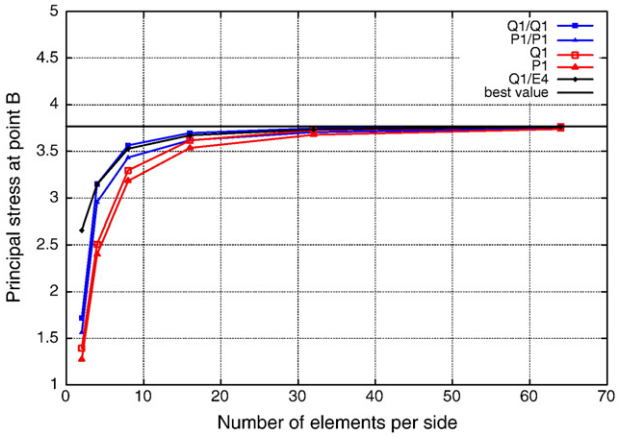

Fig. 3. Cook's membrane problem. Principal stress at point B versus number of elements along each side.

Table 2
CPU time (s) for different quadrilateral meshes and formulations in Cook's membrane problem: *Q1*, Q1/*E4*, Q1/Q1 (iterative) and Q1/Q1 (monolithic).

Mesh	Q1	Q1/*E4*	Q1/Q1 (i)	Q1/Q1 (m)
64×64	0.26	0.31	0.43	2.07
128×128	1.78	2.11	2.59	25.03
256×256	20.10	20.90	24.80	300.38

This relative increase would also be smaller using iterative solvers, first because of the lower complexity (cost increase with the number of unknowns) and, second, because the solution of a given nonlinear iteration will be a better and better guess for the linear solver as the iterative procedure goes on.

5.2. Clamped arch problem

As a further illustration of the performance of the stabilized mixed $\boldsymbol{\varepsilon}/\mathbf{u}$ formulation, we consider a clamped arch, of radius $R=10$ and thickness $t=1$, vertically loaded at the top (see Fig. 2, dimensions are in m). Because of symmetry, only one half of the structure needs to be considered. The problem has been discretized into structured meshes consisting of N finite elements along the radial direction and $10\,N$ elements in the circumferential direction. Length $L_0=t$ is taken as representative of the problem, for the evaluation of the stabilization parameters in the mixed formulation (Fig. 4).

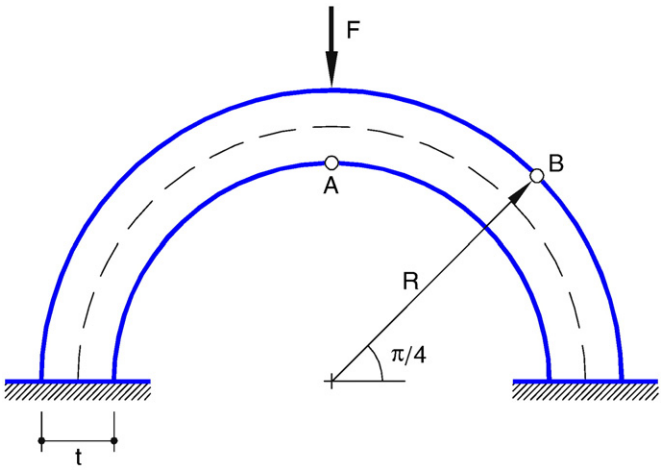

Fig. 4. Geometry for the clamped arch problem.

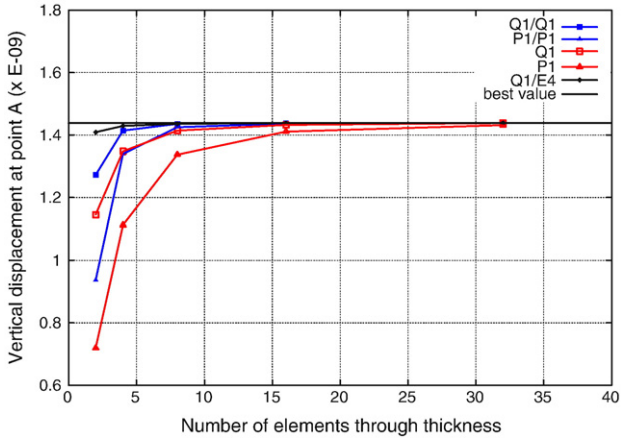

Fig. 5. Clamped arch problem. Vertical displacement of point *A* versus number of elements along the thickness.

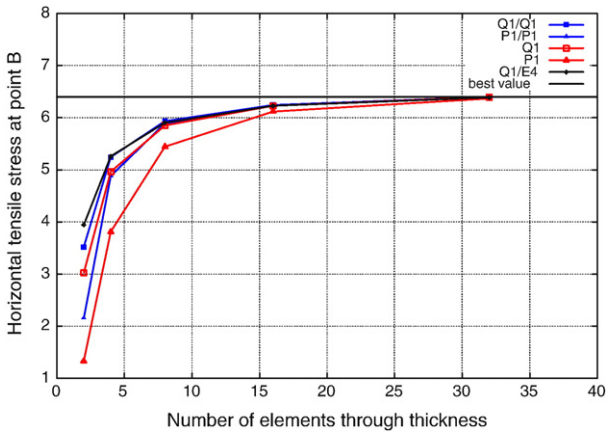

Fig. 6. Clamped arch problem. Vertical displacement of point *B* versus number of elements along the thickness.

As in the previous example, Figs. 5 and 6 compare the results obtained with five different spatial discretizations: Q1/Q1, *P*1/*P*1, *Q1*, *Q1E4* and *P1*. Fig. 5 shows the relative convergence of the five discretizations used on the computed value of the vertical displacement under the point load (point A in Fig. 2). In this case, the mixed interpolations also show improved performance over their corresponding irreducible formulations in the displacement results. The quadrilateral mixed elements also compare well with the quadrilaterals with enhanced strains, which are very accurate for all meshes.

Fig. 6 shows results on the computed value of the major principal stress at point *B* on the outer face of the arch (see Fig. 4). The values reported for the irreducible and enhanced elements correspond to the continuous projection $P_h(\mathbf{C}:\nabla^s\mathbf{u}_h)$ evaluated at the mesh nodes. Again, the mixed formulations show better accuracy that the corresponding irreducible ones. The quadrilateral mixed elements and the quadrilateral elements with enhanced strains show almost identical performance in terms of stresses.

5.3. Sharp V-notched specimen under tension

For this last example, let us consider the vertical stretching of a square V-notched specimen as the one shown in Fig. 7. Dimensions of the sample are 2×2 m×m (width×height) and the V-shaped notch has a length of 1 m and a maximum width at the boundary of 0.02 m. For the evaluation of the stabilization parameters in the mixed

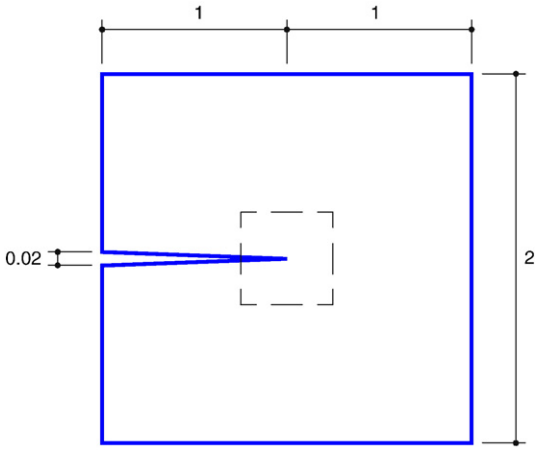

Fig. 7. Geometry for the sharp V-notched specimen under tension.

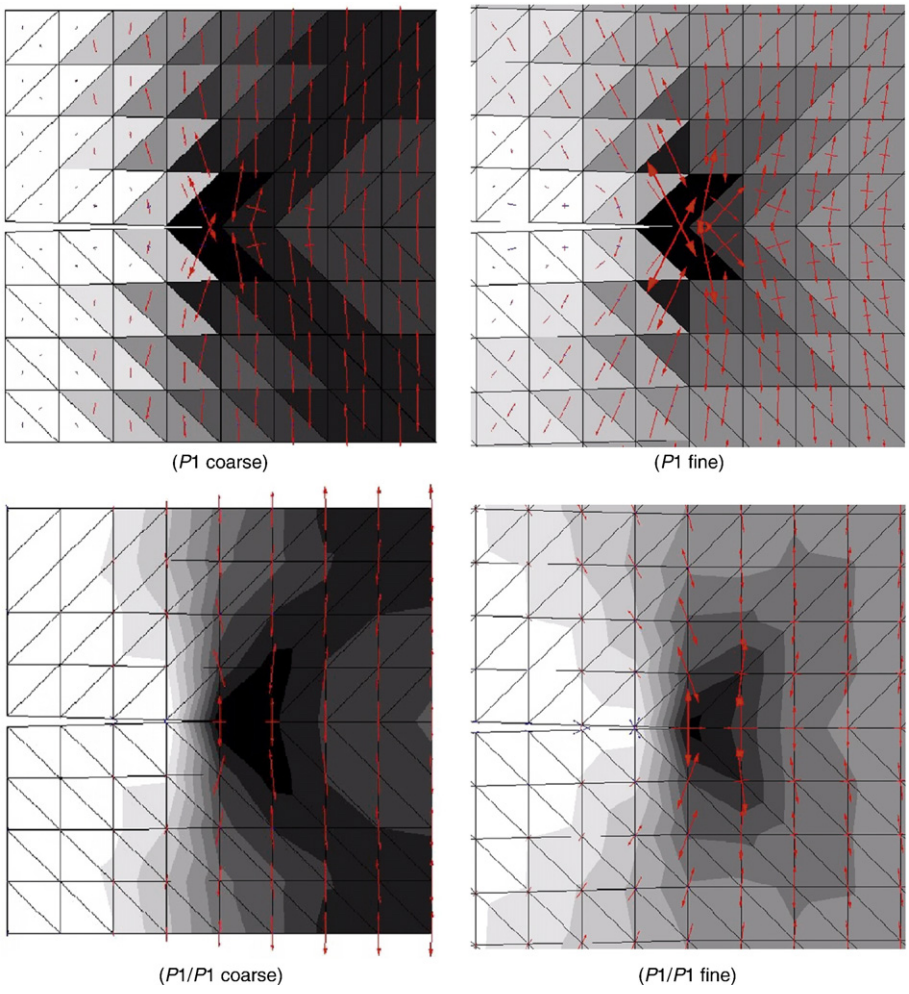

Fig. 8. Principal stresses for V-notched specimen under tension.

formulation, $L_0 = 1$ m is taken as representative length of the problem. Uniform vertical displacements of opposed sign are imposed at the top and bottom boundaries.

In the continuous elastic problem associated to this situation, the strain and stress fields are singular at the tip of the sharp notch. The discrete model corresponding to the irreducible finite element formulation performs satisfactorily in terms of a global error norm, but approximates very poorly the actual behavior near the singular points.

To show this, a coarse structured mesh consisting of $8\times8\times2$ *P1* triangles with a $\pm45°$ bias is constructed. Fig. 8 (*P1* coarse) depicts principal stresses computed on this mesh, plotted on top of the contour lines for the major principal stress value. Note the strong mesh bias dependence that is observed in front of and behind the notch tip. In fact, the largest values of the stresses occur behind the tip (left of the tip in the Figure), rather than in front of it (right of the tip in the Figure). Computed stress directions near the tip of the crack also show strong mesh bias dependence. Fig. 8 (*P1* fine) depicts principal stresses computed on a finer structured mesh consisting of $64\times64\times2$ *P1* triangles with the same $\pm45°$ bias. A zoom on the area around the tip of the crack is shown, where the same errors as in the coarse mesh are displayed. Comparing the results obtained for both meshes, it can be appreciated that the severe local errors caused by the mesh alignment are not alleviated by mesh refinement.

Fig. 8 (*P*1/*P*1 coarse) and (*P*1/*P*1 fine) show corresponding results obtained used the stabilized mixed strain/displacement formulation on the same coarse and fine meshes. The improved accuracy with respect to the irreducible formulation is clear. In particular, the maximum principal stress value is detected exactly at the tip of the notch; computed stress directions are also noticeably improved. The importance of these two features in nonlinear solid mechanics is evident. As it is shown in Part II of this work [40], they are crucial in strain localization problems where the constitutive equation depends on the principal stress values and their directions.

6. Conclusions

This paper presents the formulation of stable mixed stress/displacement and strain/displacement finite elements using equal order interpolation for the solution of nonlinear problems is solid mechanics. The proposed stabilization is based on the sub-grid scale approach and it circumvents the strictness of the compatibility conditions. The final method, consisting of stabilizing the standard formulation for mixed elements with the projection of the displacement symmetric gradient, yields an accurate and robust scheme, suitable for engineering applications in 2D and 3D. Numerical examples show that results compare favorably with the corresponding irreducible formulations, showing improved accuracy in the evaluation of the stress field. This characteristic is of great importance when facing nonlinear problems.

Acknowledgment

Financial support from the Spanish Ministry for Education and Science under the *SEDUREC* project (CSD2006-00060) is acknowledged.

References

[1] B.X. Fraeijs de Veubeke, Displacement and equilibrium models in the finite element method, in: O.C. Zienkiewicz, G. Hollister (Eds.), Stress Analysis, Wiley, 1965.
[2] D.S. Malkus, T.J.R. Hughes, Mixed finite element methods — reduced and selective integration techniques: a unification of concepts, Comput. Meth. Appl. Mech. Eng. 15 (1978) 63–81.
[3] D.N. Arnold, F. Brezzi, M. Fortin, A stable finite element for the Stokes equations, Calcolo 21 (1984) 337–344.
[4] J.C. Simo, R.L. Taylor, K.S. Pister, Variational and projection methods for the volume constraint in finite deformation elasto-plasticity, Comput. Meth. Appl. Mech. Eng. 51 (1985) 177–208.
[5] J.C. Simo, M.S. Rifai, A class of mixed assumed strain methods and the method of incompatible modes, Int. J. Numer. Meth. Eng. 29 (1990) 1595–1638.
[6] B.D. Reddy, J.C. Simo, Stability and convergence of a class of enhanced assumed strain methods, SIAM J. Num. Anal. 32 (1995) 1705–1728.
[7] J. Bonet, A.J. Burton, A simple average nodal pressure tetrahedral element for incompressible and nearly incompressible dynamic explicit applications, Commun. Numer. Meth. Eng. 1 (4) (1998) 437–449.
[8] O.C. Zienkiewicz, J. Rojek, R.L. Taylor, M. Pastor, Triangles and tetrahedra in explicit dynamic codes for solids, Int. J. Numer. Meth. Eng. 43 (1998) 565–583.
[9] R.L.A. Taylor, Mixed-enhanced formulation for tetrahedral elements, Int. J. Num. Meth. Eng. 47 (2000) 205–227.
[10] C.R. Dohrmann, M.W. Heinstein, J. Jung, S.W. Key, W.R. Witkowsky, Node-based uniform strain elements for three-node triangular and four-node tetrahedral meshes, Int. J. Numer. Meth. Eng. 47 (2000) 1549–1568.
[11] J. Bonet, H. Marriot, O. Hassan, An averaged nodal deformation gradient linear tetrahedral element for large strain explicit dynamic applications, Commun. Numer. Meth. Eng. 17 (2001) 551–561.
[12] J. Bonet, H. Marriot, O. Hassan, Stability and comparison of different linear tetrahedral formulations for nearly incompressible explicit dynamic applications, Int. J. Numer. Meth. Eng. 50 (2001) 119–133.
[13] E. Oñate, J. Rojek, R.L. Taylor, O.C. Zienkiewicz, Linear triangles and tetrahedra for incompressible problem using a finite calculus formulation, Proceedings of European Conference on Computational Mechanics, ECCM, 2001.
[14] E.A. de Souza Neto, F.M.A. Pires, D.R.J. Owen, A new F-bar-method for linear triangles and tetrahedra in the finite strain analysis of nearly incompressible solids, Proceedings of VII International Conference on Computational Plasticit, COMPLAS, 2003.
[15] O.C. Zienkiewicz, R.L. Taylor, J.A.W. Baynham, Mixed and irreducible formulations in finite element analysis, in: S.N. Atlury, R.H. Gallagher, O.C. Zienkiewicz (Eds.), Hybrid and Mixed Finite Element Methods, Wiley, 1983.
[16] O.C. Zienkiewicz, R.L. Taylor, The Finite Element Method, Butterworth-Heinemann, Oxford, 2000.
[17] M. Bischoff, K.-U. Bletzinger, Improving stability and accuracy of Reissner–Mindlin plate finite elements via algebraic subgrid scale stabilization, Comput. Meth. Appl. Mech. Eng. 193 (2004) 1517–1528.
[18] D.N. Arnold, Mixed finite element methods for elliptic problems, Comput. Meth. Appl. Mech. Eng. 82 (1990) 281–300.
[19] F. Brezzi, M. Fortin, Mixed and Hybrid Finite Element Methods, Spinger, New York, 1991.
[20] F. Brezzi, M. Fortin, D. Marini, Mixed finite element methods with continuous stresses, Math. Models Meth. Appl. Sci. 3 (1993) 275–287.
[21] D. Mijuca, On hexahedral finite element HC8/27 in elasticity, Comput. Mech. 33 (2004) 466–480.
[22] D.N. Arnold, R. Winther, Mixed finite elements for elasticity, Numer. Math. 92 (2002) 401–419.
[23] D.N. Arnold, G. Awanou, R. Winther, Finite elements for symmetric tensors in three dimensions, Math. Comput. 77 (2008) 1229–1251.
[24] T.J.R. Hughes, Multiscale phenomena: Green's function, Dirichlet-to Neumann formulation, subgrid scale models, bubbles and the origins of stabilized formulations, Comput. Meth. Appl. Mech. Eng. 127 (1995) 387–401.
[25] T.J.R. Hughes, G.R. Feijoó, L. Mazzei, J.B. Quincy, The variational multiscale method—a paradigm for computational mechanics, Comput. Meth. Appl. Mech. Eng. 166 (1998) 3–28.
[26] R. Codina, J. Blasco, A finite element method for the Stokes problem allowing equal velocity–pressure interpolations, Comput. Meth. Appl. Mech. Eng. 143 (1997) 373–391.
[27] R. Codina, Stabilization of incompressibility and convection through orthogonal sub-scales in finite element methods, Comput. Meth. Appl. Mech. Eng. 190 (2000) 1579–1599.
[28] R. Codina, Analysis of a stabilized finite element approximation of the Oseen equations using orthogonal subscales, Appl. Numer. Math. 58 (2008) 264–283.
[29] R. Codina, Finite element approximation of the three field formulation of the Stokes problem using arbitrary interpolations, SIAM J. Numer. Anal. 47 (2009) 699–718.
[30] S. Badia, R. Codina, Unified stabilized finite element formulations for the Stokes and the Darcy problems, SIAM Journal on Numerical Analysis 17 (2009) 309–330.
[31] M. Chiumenti, Q. Valverde, C. Agelet de Saracibar, M. Cervera, A stabilized formulation for incompressible elasticity using linear displacement and pressure interpolations, Comput. Meth. Appl. Mech. Eng. 191 (2002) 5253–5264.
[32] M. Cervera, M. Chiumenti, Q. Valverde, C. Agelet de Saracibar, Mixed linear/linear simplicial elements for incompressible elasticity and plasticity, Comput. Meth. Appl. Mech. Eng. 192 (2003) 5249–5263.
[33] M. Chiumenti, Q. Valverde, C. Agelet de Saracibar, M. Cervera, A stabilized formulation for incompressible plasticity using linear triangles and tetrahedra, Int. J. Plast. 20 (2004) 1487–1504.
[34] M. Cervera, M. Chiumenti, C. Agelet de Saracibar, Softening, localization and stabilization: capture of discontinuous solutions in J2 plasticity, Int. J. Numer. Anal. Meth. Geomechanics 28 (2004) 373–393.
[35] M. Cervera, M. Chiumenti, C. Agelet de Saracibar, Shear band localization via local J_2 continuum damage mechanics, Comput. Meth. Appl. Mech. Eng. 193 (2004) 849–880.
[36] M. Cervera, M. Chiumenti, Size effect and localization in J_2 plasticity, International Journal of Solids and Structures 46 (2009) 3301–3312.
[37] M. Pastor, T. Li, X. Liu, O.C. Zienkiewicz, Stabilized low-order finite elements for failure and localization problems in undrained soils and foundations, Comput. Meth. Appl. Mech. Eng. 174 (1999) 219–234.
[38] M. Mabssout, M.I. Herreros, M. Pastor, Wave propagation and localization problems in saturated viscoplastic geomaterials, Comput. Meth. Appl. Mech. Eng. 192 (2003) 955–971.
[39] M. Mabssout, M. Pastor, A Taylor–Galerkin algorithm for shock wave propagation and strain localization failure of viscoplastic continua, Int. J. Numer. Meth. Eng. 68 (2006) 425–447.
[40] Cervera, M., Chiumenti, M. and Codina, R.. Mixed stabilized finite element methods in nonlinear solid mechanics. Part II: strain localization, Comp. Meth. in Appl. Mech. and Eng. (this issue).
[41] J.K. Djoko, B.P. Lamichhane, B.D. Reddy, B.I. Wohlmuth, Conditions for equivalence between the Hu–Washizu and related formulations, and computational behavior in the incompressible limit, Comput. Meth. Appl. Mech. Eng. 195 (2006) 4161–4178.
[42] R. Codina, J. Principe, J. Baiges, Subscales on the element boundaries in the variational two-scale finite element method, Comput. Meth. Appl. Mech. Eng. 198 (2009) 838–852.
[43] Badia, S. and Codina, R. Stabilized continuous and discontinuous Galerkin techniques for Darcy flow, Comp. Meth. Appl. Mech. Eng. 199 (2010) 1654–1667. E-prints UPC: http://upcommons.upc.edu/e-prints/handle/2117/2447.
[44] R. Codina, Stabilized finite element approximation of transient incompressible flows using orthogonal subscales, Comput. Meth. Appl. Mech. Eng. 191 (2002) 4295–4321.
[45] C. Baiocchi, F. Brezzi, L. Franca, Virtual bubbles and Galerkin/least-squares type methods (Ga.L.S.), Comput. Meth. Appl. Mech. Eng. 105 (1993) 125–141.
[46] F. Brezzi, M.O. Bristeau, L. Franca, M. Mallet, G. Rogé, A relationship between stabilized finite element methods and the Galerkin method with bubble functions, Comput. Meth. Appl. Mech. Eng. 96 (1992) 117–129.
[47] E.P. Kasper, R.L. Taylor, A mixed-enhanced strain method. I: Geometrically linear problems. II: Geometrically nonlinear problems, Comput. Struct. 75 (2000) 237-250, 251-260.
[48] Cervera, M., Agelet de Saracibar, C. and Chiumenti, M. COMET: COupled MEchanical and Thermal analysis. Data Input Manual, Version 5.0, Technical report IT-308, http://www.cimne.upc.es, 2002.
[49] GiD: The personal pre and post preprocessor. http://www.gid.cimne.upc.es, 2002.